# *Interlaminar Fracture Toughness of Laminated Woven Composites Reinforced with Aligned Nanoscale Fibers: Mechanisms at the Macro, Micro, and Nano Scales*

# Interlaminar Fracture Toughness of Laminated Woven Composites Reinforced with Aligned Nanoscale Fibers: Mechanisms at the Macro, Micro, and Nano Scales

Sunny S. Wicks[1] and Brian L. Wardle[2]
*Massachusetts Institute of Technology, Cambridge, MA, 02139*

**Several hybrid architectures with aligned nanoscale fibers have been shown to provide inter- and intra-laminar reinforcement of fiber reinforced polymer composites. In one architecture, aligned carbon nanotubes (CNTs) grown on advanced fibers in a woven ply creates a 'fuzzy fiber' reinforced plastic (FFRP) laminate. Here the mechanisms of Mode I fracture toughness enhancement are elucidated by varying the type of epoxy and reinforcing CNT length experimentally. Reinforcement effects are shown to vary from reduced initiation toughness to more than 100% increase in steady-state fracture toughness, depending upon the multi-scale interlaminar fracture mechanisms. Fracture-surface morphology investigations using several techniques reveal that interlaminar toughness enhancement for an aerospace infusion resin is significantly less than that for a hand lay-up marine epoxy. Long (~20 micron) aligned CNTs toughens significantly (> 1 kJ/m$^2$ increase for marine epoxy) by driving the crack through tortuous paths around and through tows, whereas shorter CNTs produce less toughening (or even reduced toughness in aerospace epoxy), which is attributed to shorter pullout lengths and grown-CNT morphology differences. These findings reveal for the first time the multiscale nature of the composite ply interface, and the mechanisms at work at the chemical, nano, and micro scales that influence the macroscopic behavior. Extensions and future work are discussed, including preliminary results using the multifunctional attributes of the nanoengineered composite for structural health monitoring (SHM) concomitant with interlaminar fracture testing.**

**Nomenclature**

| | | |
|---|---|---|
| *CNT* | = | carbon nanotube |
| *CVD* | = | catalyst vapor deposition |
| *DCB* | = | double cantilever beam |
| $G_{Ic}$ | = | Mode I interlaminar fracture toughness |
| *FFRP* | = | fuzzy fiber reinforced plastic |
| *FRP* | = | fiber reinforced plastic |
| *RTM* | = | resin transfer molding |
| *VARI* | = | vacuum assisted resin infusion |
| *WS* | = | West Systems (marine) epoxy |

## I. Introduction

AEROSPACE structural components are increasingly being made of fiber reinforced plastics (FRPs) due to their excellent mass-specific mechanical properties. While properties in the plane of the fibers are strong, stiff, and tailorable, the interlaminar region is relatively weak and compliant, leading to failure due to delamination and other damage modes. To address these deficiencies at the interlaminar interface, several architectures have been developed to reinforce strength and toughness properties in the through-thickness direction of the laminate, including Z-pinning, stitching, and 3-D weaving.[1] These processes can result in a significant reduction in in-plane properties of the laminate plane due to damage from insertion of through-thickness direction reinforcements (hundreds of microns in diameter) and loss of fiber volume fraction in the in-plane directions.[2,3] Alternative routes to

[1] Doctoral Student, Department of Aeronautics and Astronautics, and AIAA Member.
[2] Associate Professor, Department of Aeronautics and Astronautics, and AIAA Associate Fellow.

increasing interlaminar toughness include modification of matrix properties through added toughening agents, compliant interlayers, or particles[4] and nanofibers, including in particular carbon nanotubes (CNTs) that possess advantaged specific stiffness and strength.[5,6]

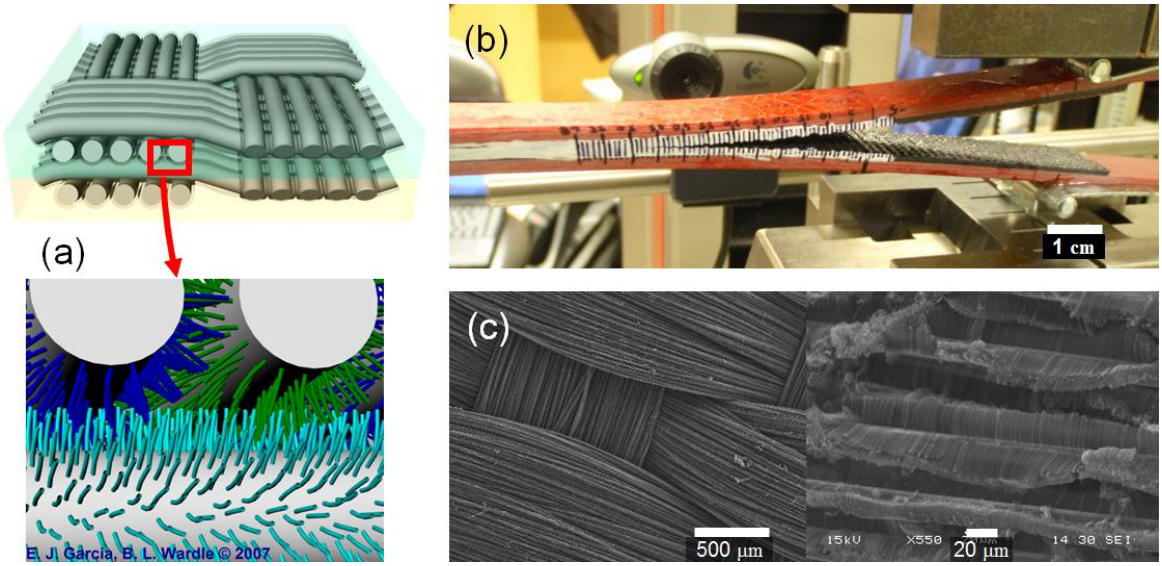


**Figure 1. Fuzzy Fiber Reinforced Plastics (FFRP)** *(a) Illustration of FFRP architecture, (b) FFRP DCB test specimen, with dimensions of 0.8" x 7" (20 x 180 mm), (c) ~20 μm long aligned CNTs on the surface of fibers in a woven alumina cloth 'fuzzy fiber' ply with aligned CNTs.*

In this paper, aligned carbon nanotubes (CNTs) are implemented in a three-dimensionally reinforced nano-engineered composite. Many approaches to CNT incorporation have been explored in the literature, including depositing CNTs on surfaces of advanced fibers, or mixing CNTs in polymer matrices before infiltration.[7-10] The aligned carbon nanotubes in this work are grown on the surfaces of fibers, termed 'fuzzy fibers' and shown in Fig. 1a, and extend across interlaminar and intralaminar regions to provide mechanical reinforcement. The CNTs are grown *in situ*, providing control of alignment and distribution while allowing easy manufacturing with low viscosity matrix systems.[11] The micron-scale diameter fibers are alumina, serving as a model system for this and several studies, because the CNT growth process does not damage the alumina fibers,[12] an effect observed by many researchers for carbon fibers.[13]

Prior work has examined the fracture toughness of coarse weave composites[11] made by hand lay-up with a two-part West Systems marine epoxy, which exhibited a 76% increase in steady-state toughness, confirming the potential for mechanical reinforcement with aligned CNTs. Manufacturing techniques were developed for flatter weave alumina cloth with an aerospace epoxy (RTM6 by Hexcel), an advanced engineering epoxy designed with low viscosity and long working times for resin transfer molding (RTM).[14] This paper continues this study on flat weave composites by isolating the role of the type of epoxy on the potential for toughness reinforcement by aligned CNTs. Mode I double cantilever beam (DCB) laminates were manufactured and tested with both the (more brittle) aerospace epoxy and the tougher marine epoxy to understand the role of the epoxy interaction with both fibers and CNTs on the multi-scale fracture mechanisms.

## II. Experimental Details

Laminates 8 plies thick, like the Mode I DCB laminates pictured in Fig. 1b, are manufactured by first producing 'fuzzy fiber' plies and then adding the epoxy into the matrix of the laminate via either hand lay-up or vacuum assisted infusion (see Fig. 2 for illustrations). Aligned CNTs are grown on 2"x7" plies of alumina ceramic cloth (Cotronics Ultra-Temp 391) by chemical vapor deposition under helium, hydrogen, and ethylene, and is described in detail elsewhere.[11,15] CNT length is controlled by varying the length of ethylene exposure. The plies in this set are made with 3 minutes of ethylene exposure, yielding CNTs that are approximately 19 μm long. Images of a fuzzy ply and aligned CNT forests are shown in Fig. 1c.

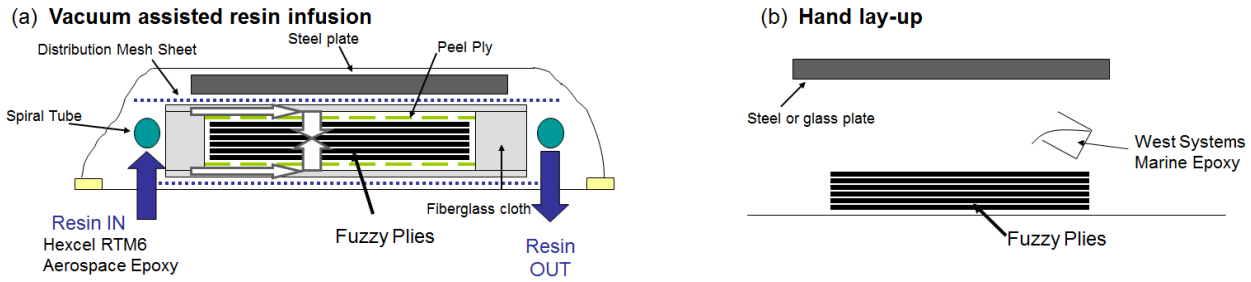


**Figure 2. Manufacturing routes for FFRP production.** *(a) Side schematic of infusion setup showing primary epoxy flow path. (b) Hand lay-up for viscous epoxy systems.*

Vacuum assisted resin infusion (VARI) is used to manufacture both FFRP and baseline (without CNTs) laminates with unmodified aerospace infusion resin (Hexcel RTM6). A schematic in Fig. 2a shows the VARI setup, where spiral tubes and distribution mesh sheets draw the epoxy along and into the laminate. The laminate is layered by porous Teflon peel ply, woven fiberglass, and distribution mesh sheets on both surfaces, and then sandwiched between steel and glass plates to ensure a flat and uniform part. A 50.8mm (2 inch) wide steel plate that matches the width of the laminate is placed on top of the stack to minimize 'racetracking' of the epoxy along the edges during infusion. This allows the vacuum bag to conform to the top plate and the edges of the laminate. Prior to infusion, the plates and laminate stack are heated under vacuum to 150°C (300°F) for two hours to displace any residual moisture. Then, the RTM6 epoxy is degassed at 80°C, and slowly drawn into the laminate at 90°C. The inlet and outlet of system is then closed off and cured at 160°C and postcured at 180°C.

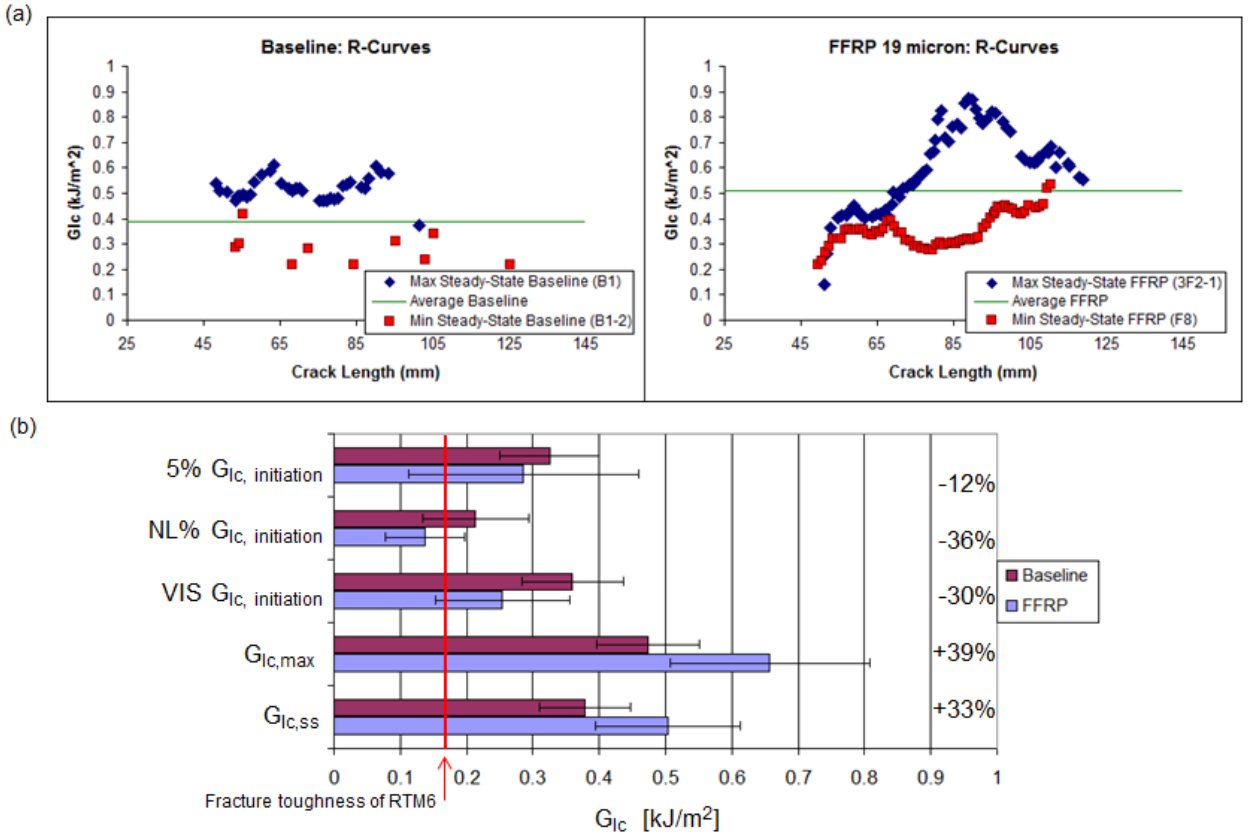


**Figure 3. Mode I Fracture Toughness of RTM6 laminates.** *(a) R-curves of Baseline and FFRP tests. (b) Fracture toughness comparison summary based on 14 baseline and 11 FFRP laminates, including manufacturer-quoted RTM6 fracture toughness of 0.168 kJ/m*$^2$*.* [16]

Hand lay-up is used with viscous epoxy systems to produce both baseline and FFRP laminates. In hand lay-up, a 2-part marine epoxy (West Systems Resin 105 and Hardener 206) is mixed and poured on to a flat surface. As shown in Fig. 2b, a ply is then laid down in the epoxy pool, and epoxy wicks into the interior of the ply. More epoxy

is poured on top, and the process is repeated until the entire laminate stack is wet. The stack is then compressed between two plates wrapped in vacuum bagging film, and left to cure for 24 hours.

To fabricate double cantilever beam (DCB) laminates for the assessment of the Mode I interlaminar fracture toughness, $G_{Ic}$, a release film is placed between the middle two plies on the last 2 inches on one end of the laminate during lay-up, to form a starter crack location at the laminate centerline. The resulting laminates are cut into 20 millimeter-wide specimens. To prevent excessive bending, 3.2 mm thick red fiberglass plates, cut to the same width of the laminate, are used to sandwich the laminates.[11] The surfaces of the laminate and fiberglass are roughened with sand paper and cleaned with acetone, isopropanol, and methanol to prepare the surfaces for bonding. A 30 minute epoxy is used to glue the fiberglass plates and hinges to the samples.

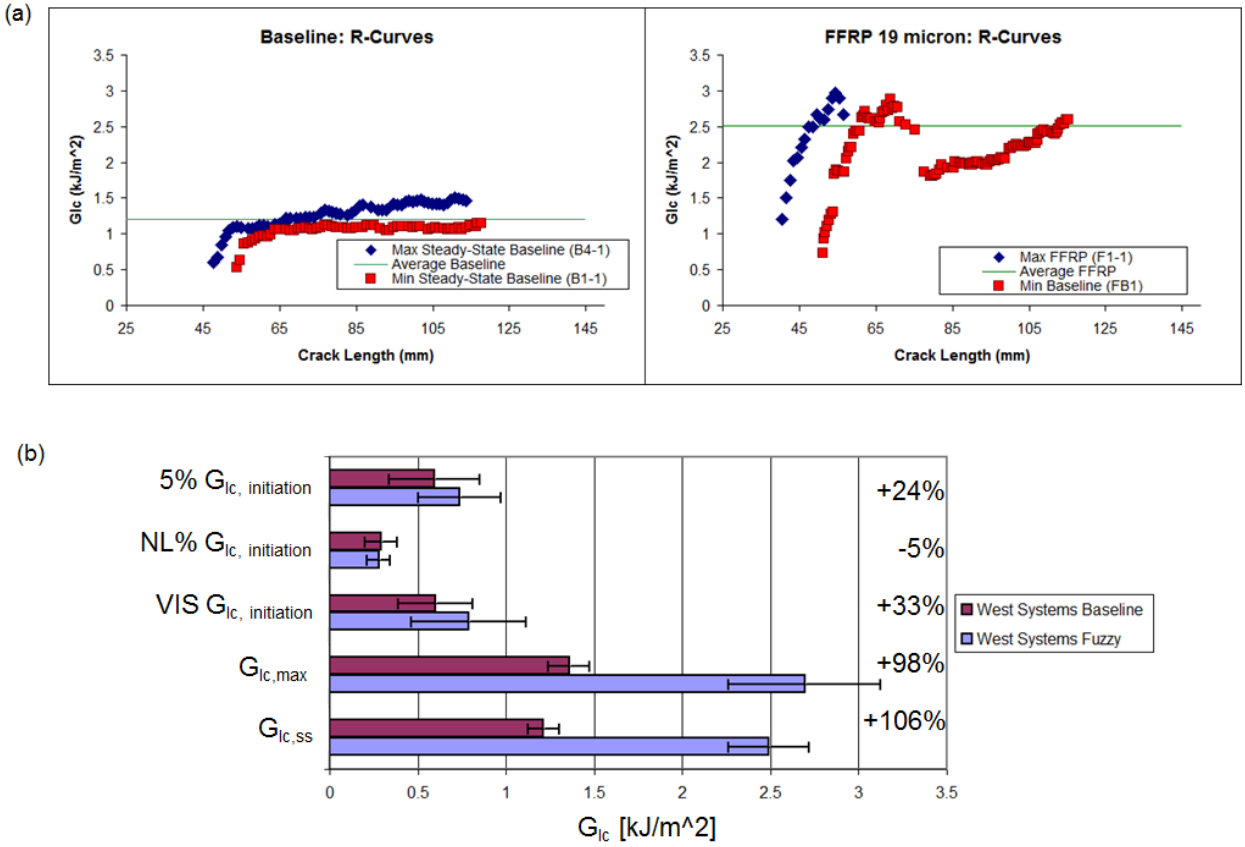


**Figure 4. Mode I Fracture Toughness of marine epoxy laminates.** *(a) R-curves of Baseline and FFRP tests. (b) Fracture toughness change summary based on 9 baseline and 19 FFRP laminates.*

## III. Results and Discussion

The fracture toughness, $G_{Ic}$, for each laminate type was calculated using the Compliance Calibration Method, as outlined in the testing standard.[17] Three measures of initiation toughness, steady state toughness, as well as the maximum observed toughness are computed. The initiation toughness, $G_{Ic,\ initiation}$ was assessed by three different methods also as defined by the ASTM standard using the point of visual propagation, deviation from linearity, and a 5% offset from linearity. The steady state toughness was taken as the average of the whole R curve excluding the first 5 points. Because the standard provides no formula to present steady state toughness when the R curves do not plateau, the comparison of the maximum $G_{Ic}$ value is also presented. The final results for the aerospace epoxy laminates are summarized in Fig. 3, and a few differences in the R curves can be seen between the baseline and FFRP plots. The baseline curves exhibit minimal toughening after crack initiation while the FFRP curves exhibit a lower initiation toughness followed by clear toughening behavior. Additionally, half of the FFRP samples continued to toughen as the crack progressed. Fig. 3b summarizes the average $G_{Ic}$ values comparing the baseline and FFRP toughness values. A moderate reduction (12-36% across all three measures) in initiation toughness is observed for these aerospace resin FFRP laminates, whereas there is a moderate, but larger, increase in both steady-state and maximum toughness.

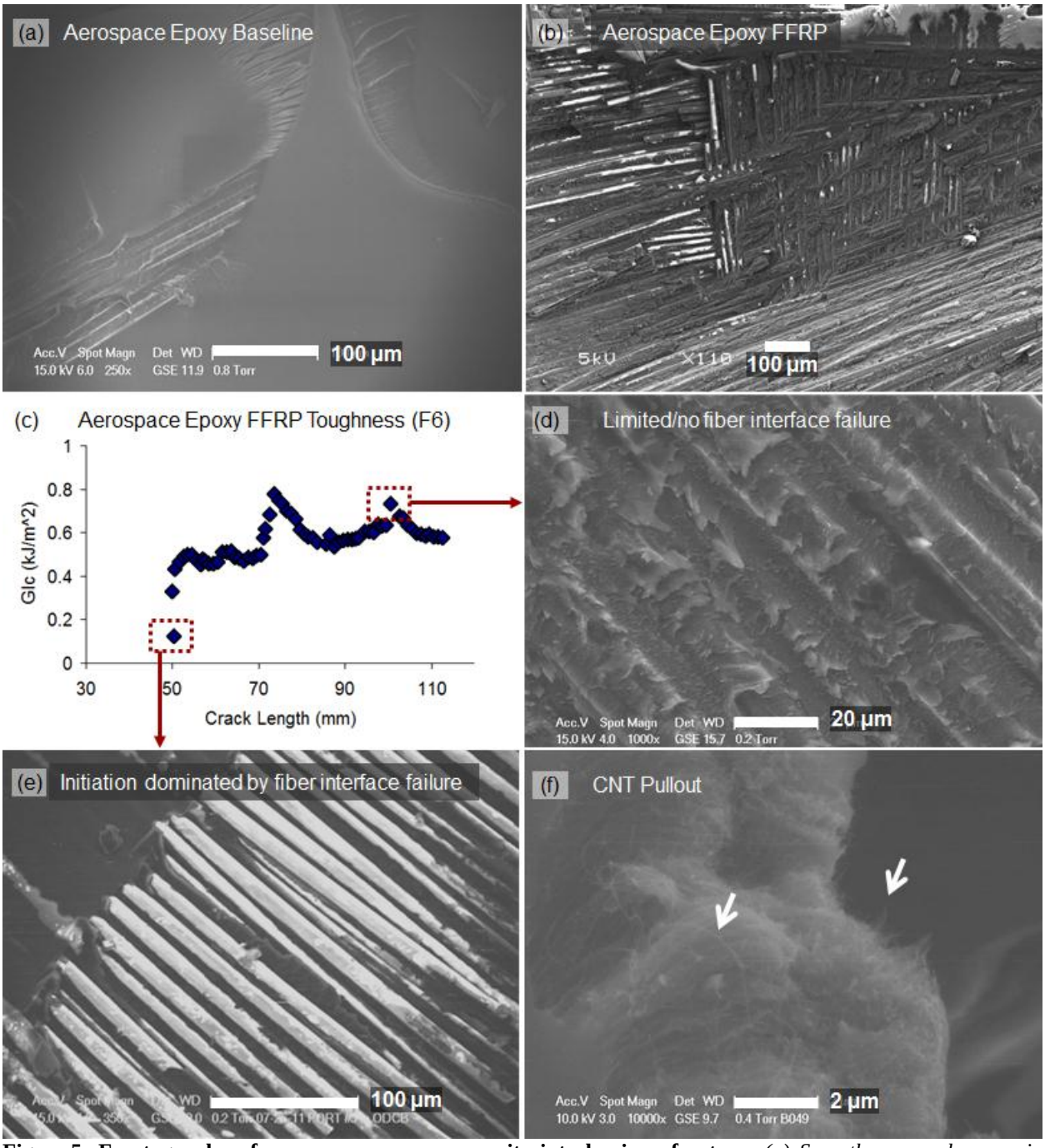


**Figure 5. Fractography of aerospace epoxy composite interlaminar fracture**. *(a) Smooth epoxy cleavage in epoxy of baseline laminates. (b) Rough epoxy along fibers in FFRP laminates. (c) Example FFRP laminate with evolving fracture toughness and multiple toughening events. (d) Matrix cohesive failure in peak toughness regions of FFRP (e) Fiber-matrix interface adhesive failure in initiation region of crack propagation. (f) CNTs pulled out of fracture surface in FFRP laminates.*

Mode I fracture toughness results of marine epoxy laminates are summarized in Fig. 4. Unlike the R-curves in the aerospace resin laminates in Fig. 3, both the baseline and FFRP laminates exhibit a rise from a low initiation value to steady-state as the crack propagates, *i.e.*, classic toughening behavior. The baseline laminates fracture consistently, reaching steady state in 10 mm. The FFRP laminates behave in two ways, either toughening for 15 mm until peaking or toughening over the entire length of the sample, unless terminated prematurely by failure of the bond between the red fiberglass tabs and the sample. Changes in initiation, steady-state, and maximum fracture

toughness are summarized in Fig. 4b where a 100% increase in toughness after initiation is observed. Specimens that terminated prematurely due to tab bond failure were not included in the $G_{Ic,max}$ or $G_{Ic,ss}$ averages before reaching a steady state value, due to tab bond failure, were not included in the $G_{Ic,ss}$ average. $G_{Ic,max}$ is based on 14 specimens, not including tests that failed before 20 mm of propagation without peaking, and $G_{Ic,ss}$ is based on 9 specimens that reached a peak value and did not follow the linear toughening trend like the sample in Fig. 6c.

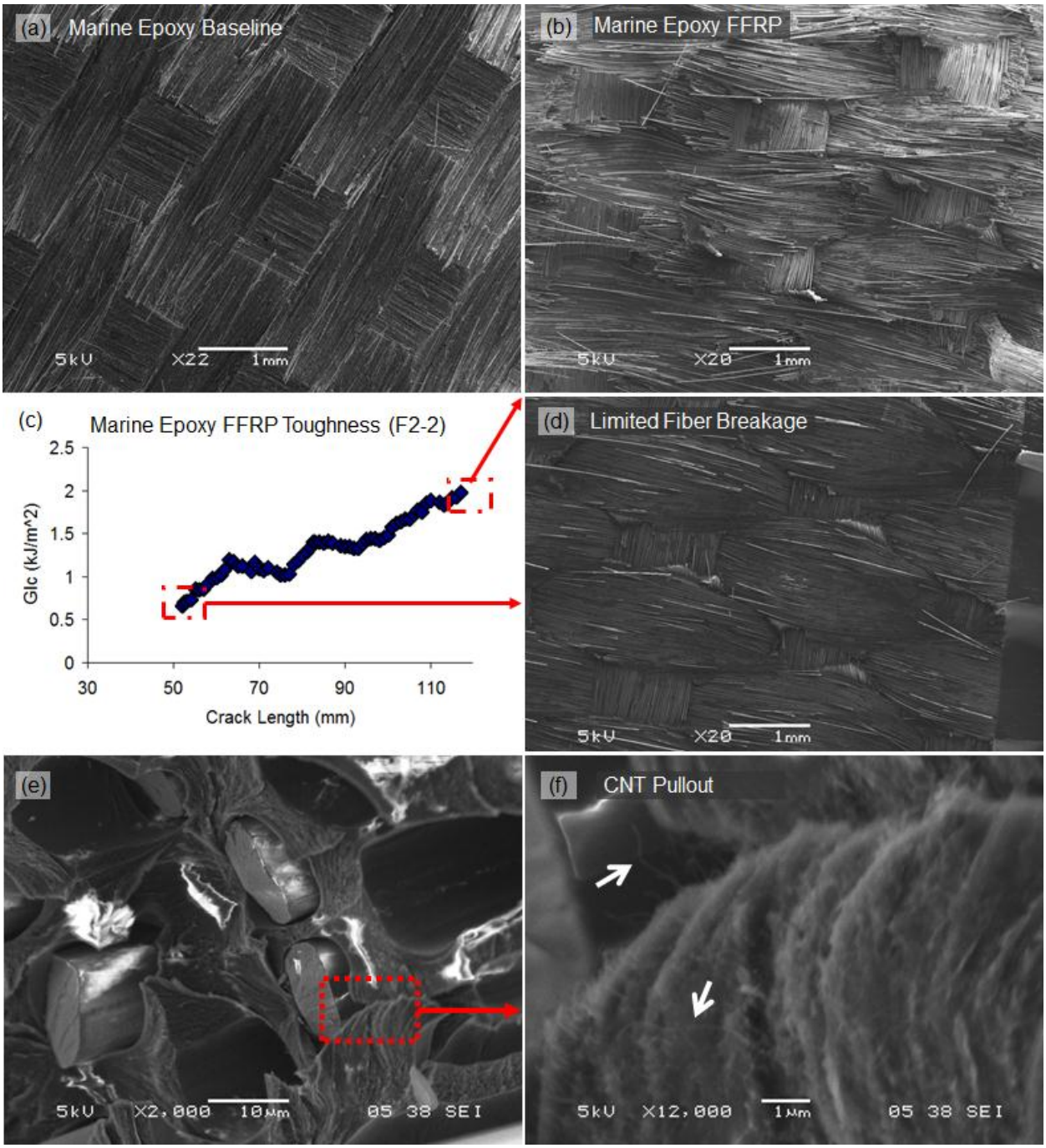


**Figure 6. Fractography of marine epoxy composite interlaminar fracture.** *(a) Individual (micro)fibers pulled out of fracture surface in baseline laminates. (b) Tow breakage and fiber pull-out in FFRP laminates. (c) Example FFRP toughness R-Curve for a laminate with increasing toughening. (d) Minimal fiber pullout in fracture surface of initiation region. (e) Broken tow surface revealing broken fibers and holes from (micro)fiber pull-out. (f) Rough CNT-filled fracture of epoxy between fibers.*

In both the aerospace and marine epoxy laminates, SEM analysis shows that the CNTs in the FFRP laminates induce microscale changes to the fracture surface. In aerospace epoxy baseline laminates, as shown in Fig. 5a, the fracture surface is dominated by smooth epoxy regions with some exposed fibers. In contrast, the fracture surface of FFRP laminates, shown in Fig. 5b, shows a very different morphology, with a rougher fracture surface as the crack follows the tows exposing some fiber surfaces with a mixture of fiber-epoxy interface adhesive failure and matrix cohesive failure. Fractography further reveals the relation between fracture morphology and variations in laminate toughness within the same laminate as shown in Fig. 5c. The fracture surfaces corresponding to the toughest regions of the laminate are dominated by matrix cohesive failure, creating rough, jagged surfaces as seen in Fig. 5d. Exposed in the rough surfaces of the matrix cohesive failure are CNTs that were pulled out, up to a few microns, during crack propagation as shown in Fig. 5f. Conversely, bare exposed fibers are observed in the initiation fracture surface in Fig. 5e where toughness is lowest. The causes for evolution of fracture morphology that governs whether the fracture remains in the matrix or follows the fiber surfaces might include local nesting or prevented nesting of the woven cloth at initiation by the release film precrack, variation in the CNT morphology along the laminate, among others.

The fracture surfaces of the marine epoxy laminates highlight a major difference between the epoxy systems. Both aerospace and marineepoxy laminates fracture show widespread fiber-matrix interface failure (see Fig. 6a and b, contrasted to the morphology of the toughest regions of aerospace epoxy FFRP as discussed above in Fig. 5d). Fiber-matrix interface failure leaves portions of the fracture surface exposed and smooth, indicating that the prevention of debonding at the fiber surface is not required for interlaminar reinforcement. Instead, increased toughness in marine epoxy laminates manifests in increased fiber and tow breakage which can be observed during crack propagation as these fibers are pulled free from the surrounding matrix and bridge across the crack tip. Increasing toughness in the FFRP laminates as seen in Fig. 6b-d correspond directly to increased (micro)fiber breaks in the fracture morphology. This fracture morphology suggests that the CNTs increase the toughness of the interlaminar region by creating a tortuous path, even to the extreme such that the crack tears through the surface of the weave rather than propagating around each tow. The oddly linear transformation from initiation to increasing toughness (limited by the laminate specimen test length) could be caused by variations in weave nesting along the crack length, which is prevented at initiation of all baseline and FFRP laminates and could vary along the length of the sample depending how adjacent plies line up. In addition to pullout and bridging of microscale fibers, the broken epoxy between fibers reveals pullout and bridging of nanoscale CNTs, indicating toughening at multiple length scales (Fig. 6e and f). Therefore CNTs change the microscale fracture behavior not necessarily by only changing mechanical properties of the matrix but also by altering the failure path and the fracture surface texture, adding surface area through fiber and CNT pullout and failure.

Macroscale differences between baseline and FFRP laminates,for both epoxy types, become apparent during crack propagation. The CNTs grown on the fiber surfaces within each tow help push apart the fibers causing the tow to swell, allowing for tows on opposite plies to nest and create a tortuous path for the crack to follow. This can be clearly observed during testing of both aerospace and marine laminates as the baseline specimens create a flat interlaminer crack while the FFRP crack propagation typically follows a wavy path. In the marine epoxy laminates, toughening seen in baseline laminates can be observed with single fibers bridging across the crack tip, while in FFRP, both single fibers and whole tows can be seen. The role of aligned CNTs creating macroscale differences in

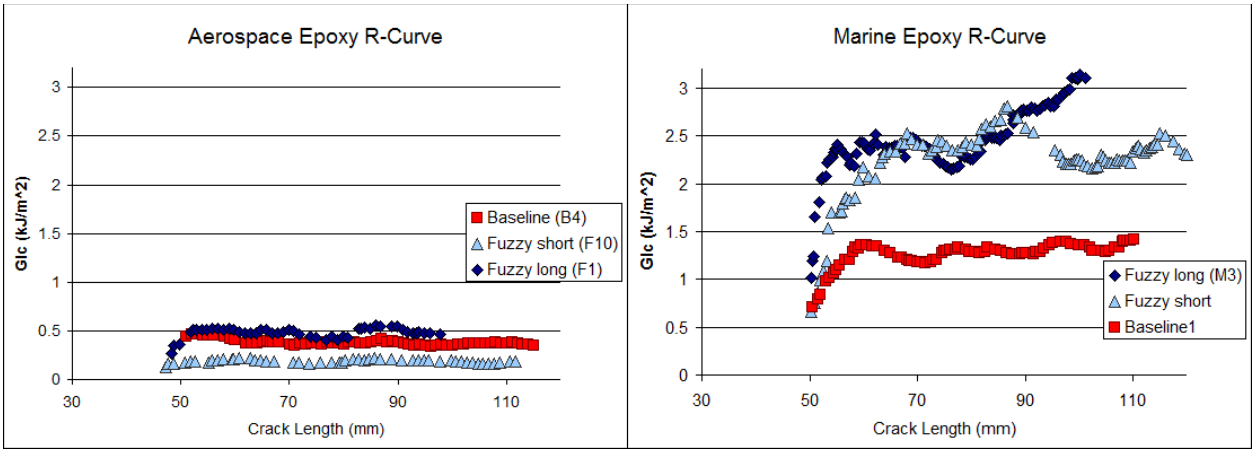


**Figure 7. Preliminary exploration of role of CNT length on laminate toughness for both aerospace and marine epoxy types. Short CNTs average 6 microns in length while long CNTs average 19.**

the tow size and interlaminar geometry vs. changing matrix material properties is being further investigated through varying the CNT length in subsequent interlaminar tests. Short aligned CNTs on the order of 6 microns in fuzzy fiber plies cover each fiber in a uniform annulus of CNTs that will spread fibers apart in the tow, but not to the extent of longer CNT 'mohawk' morphology[15] forests as can be seen in Fig. 1c. This tunable length provides control over the geometrical fiber arrangement while still reinforcing the a matrix, and can lead to counterintuitive changes in fracture toughness (see Fig. 7). An initial exploration of short CNTs in the aerospace epoxy revealed a drastic drop in toughness compared to the baseline while short CNTs in marine epoxy provide significant toughening, highlighting the need to understand the mechanism by which CNT reinforcement influences crack propagation. When applying the fuzzy fiber architecture to a chosen fiber and matrix system, the dependence of toughness on the CNT length and polymer type will need to be established for tailoring interlaminar toughness. This leads to intriguing possibilities for sizing of the nanoscale CNT fibers as well.

## Conclusion

The addition of aligned CNTs has been shown to improve the steady state Mode I fracture toughness of laminated composites. Fractography reveals toughening mechanisms for both aerospace and marine epoxy laminates at several length scales, from the pull-out of carbon nanotubes to inducing tow breakage. The toughening behavior and magnitude of steady-state toughness improvement, however, is dependant on the type of epoxy. In the more brittle aerospace epoxy laminate, modest improvement in steady-state toughnesses with long CNTs are made possible by maintaining cohesive matrix failure through tight interlaminar regions around woven tow features while increasing fracture surface area through CNT pullout and epoxy fracture. The tougher marine epoxy allows large improvements with long CNTs by maintaining fiber-matrix interface failure while significantly adding instances of fiber breakage and pullout along with CNT pullout and epoxy fracture. Varying the CNT length begins to reveal how the geometrical arrangement of fibers through tow swelling and changes in nesting affect the crack propagation path and subsequent interlaminar toughness.

The clarification of multi-scale toughening modes in this work will be supplemented through future studies establishing the extent to which nanoscale reinforcement toughens the matrix only (i.e. no fibers) and isolating the role and mechanisms of the CNT-matrix interface in resisting crack growth, leading to an understanding of how the choice of epoxy and fiber type dictate the magnitude of improvement possible. The alumina FFRP system studied is a useful model system to study features of aligned CNT property tailoring that are isolated from fiber damage due to CNT growth. However, a more engineering relevant system is carbon FFRP, particularly for aerospace applications. Future work will include study of carbon FFRP laminate interlaminar and intralaminar studies, based on recent work demonstrating synthesis of CNTs on carbon fibers that minimizes deleterious damage to the fibers.[18] Last, incorporation of a continuous network of aligned CNTs enables not only mechanical reinforcement but also damage detection by creating electrically conductive sensors for damage detection,[19] allowing real-time tracking of damage progession through changes in resistivity as microcracking and delamination disrupts the conductive network. Preliminary testing combining resistance-based damage detection with Mode I fracture testing has demonstrated the feasibility of this approach (see Fig. 8), and indeed has shown a prognostic capability.

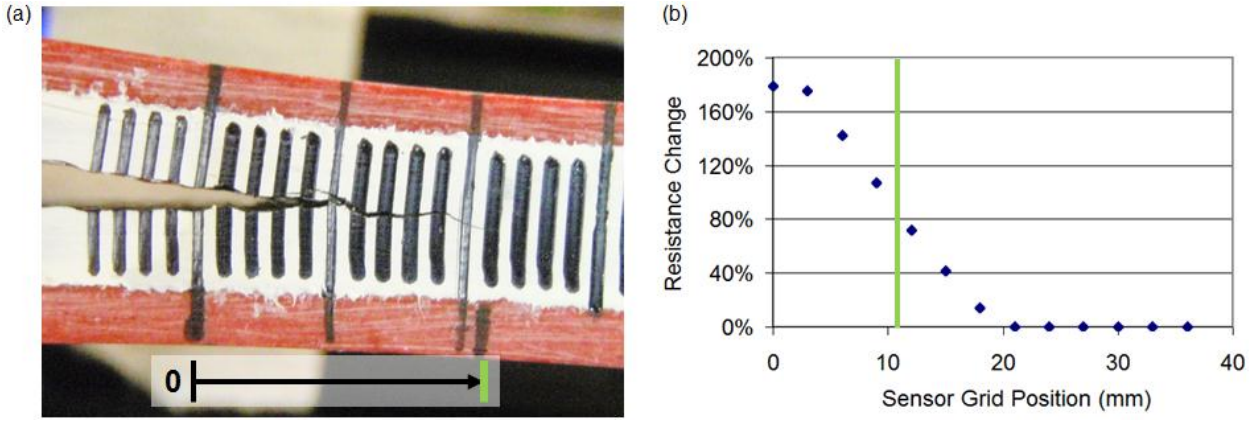


**Figure 8. In situ damage sensing during in Mode I DCB tests**. *(a) Side view of laminate with visual crack tracking, each tick mark represents* 1 mm*. (b) Relative electrical resistance change as measured through laminate thickness during test. Green line represents corresponding visual crack tip position.*

## Acknowledgments

This work was supported by Airbus S.A.S., Boeing, Embraer, Lockheed Martin, Saab AB, Textron Inc., Composite Systems Technology, Hexcel, and TohoTenax through MIT's Nano-Engineered Composite aerospace STructures (NECST) Consortium. Sunny Wicks is supported by the NASA Space Technology Research Fellowships (NSTRF) and MIT's Linda and Richard (1958) Hardy Fellowship. The authors thank John Kane and the entire necstlab at MIT for technical support and advice, Hexcel for materials donation, Metis Design for multifunctional testing. This work made use of the MRSEC Shared Experimental Facilities at MIT, supported by the National Science Foundation under award number DMR-08-19762.

## References

[1] Tong, L., Mouritz, A.P., and Bannister, M.K., "*3D Fibre Reinforced Polymer Composites*". Oxford, 2002.

[2] Dransfield, K.A., Jain, L.K., and Mai, Y.-W., "On the effects of stitching in CFRPs—1. Mode I delamination toughness," *Composites Science and Technology*, Vol. 58, pp. 815-827, 1998.

[3] Partridge, I.K., and Cartie, D.D.R., "Delamination Resistant Laminates by Z-Fiber_Pinning: Part I Manufacture and Fracture Performance," *Composites Part A*, Vol. 36, No. 1, 2005, pp. 55–64.

[4] Böger, L., Sumfleth, J., Hedemann, H., and Schulte, K., "Improvement of fatigue life by incorporation of nanoparticles in glass fibre reinforced epoxy". *Composites Part A: Applied Science and Manufacturing*, Vol. 41, No. 10, 2010, pp. 1419-1424.

[5] Salvetat, J.P., Kulik, A.J., Bonard, J.M., et al., "Elastic modulus of ordered and disordered multiwalled carbon nanotubes". *Advanced Materials*, Vol. 11, No. 2, 1999, pp. 161–5.

[6] Coleman., J.N., Khan, U., Blau, W.J., and Gun'ko, Y.K., "Small but strong: A review of the mechanical properties of carbon nanotube-polymer composites," *Carbon*. Vol. 44, No. 9, 2006, pp. 1624-1652.

[7] Bekyarova, E., Thostenson, E.T., Yu, A., Kim, H., et al., "Multiscale Carbon Nanotubes for Carbon Fiber Reinforcement for Advanced Epoxy Composites". *Langmuir*, Vol. 23, No. 7, 2007, pp. 3970-3974.

[8] Godara, A., Mezzo, L., Luizi, F., Warrier, A., et al., "Influence of carbon nanotube reinforcement on the processing and the mechanical behaviour of carbon fiber/epoxy composites," *Carbon*, Vol. 47, pp. 2914-2923.

[9] Chou, T.-W., Gao, L., Thostenson, E.T., Zhang, Z., and Byun, J.-H., "An assessment of the science and technology of carbon nanotube-based fibers and composites," *Composites Science and Technology*, Vol. 70, No. 1, pp. 1-19.

[10] Chandrasekaran, V., Advani, S., and Santare, M., "Role of processing on interlaminar shear strength enhancement of epoxy/glass fiber/multi-wallec carbon nanotube hybrid composites," *Carbon*, Vol. 48, No. 13, 2010, pp. 3692-3699.

[11] Wicks, S.S., Guzmán de Villoria, R., and Wardle, B.L., "Interlaminar and intralaminar reinforcement of composite laminates with aligned carbon nanotubes". *Composites Science and Technology*, Vol. 70, pp 20-28, 2010.

[12] Garcia, E.J., Hart, J., and B.L. Wardle, "Long Carbon Nanotubes Grown on the Surface of Fibers for Hybrid Composites," *AIAA Journal*, Vol. 46, No.6, 2008, pp.1405-1412.

[13] Qian, H.; Bismarck, A.; Greenhalgh, E. S.; Kalinka, G., et al., "Hierarchal Composites Reinforced with Carbon Nanotube Grafted Fibers: The Potential Assessed at the Single Fiber Level," Chemistry of Materials, Vol. 20, 2008, pp. 1862-1869.

[14] Lidston D., Wicks, S., and Wardle, B.L., "Factors Controlling Infusion Processing of Laminated Composites Containing Aligned Carbon Nanotubes", *Proceedings of the 52nd AIAA/ASME/ASCE/AHS/ASC Structures, Structural Dynamics, and Materials Conference*, Denver, CO, April 4-7, 2011.

[15] Yamamoto, N., Hart, A.J., Garcia, E.J., et al., "High-yield growth and morphology control of aligned carbon nanotubes on ceramic fibers for multifunctional enhancement of structural composites". *Carbon*, Vol. 47, No. 3, pp 551–560, 2009.

[16] http://www.hexcel.com/Resources/DataSheets/RTM-Data-Sheets/RTM6_global.pdf

[17] ASTM D 5528-01. "Standard Test Method for Mode 1 Interlaminar Fracture Toughness of Unidirectional Fiber-Reinforced Polymer Matrix Composites," ASTM International.

[18] Steiner III, S. A. (2011). *Carbon nanotube Growth on Challenging Substrates: Applications for Carbon-Fiber Composites.* Ph.D. Thesis. Massachusetts Institute of Technology: U.S.A.

[19] Guzmán de Villoria, R., Yamamoto, N. et al. "Multi-physics damage sensing in nano-engineered structural composites". *Nanotechnology*, Vol. 22, No. 18, p 185502, 2011.